Measurement of the $\gamma + D^{*\pm}$ Cross Section in $\bar{p}p$ Collisions at $\sqrt{s} = 1.8$ TeV

F. Abe,[15] H. Akimoto,[34] A. Akopian,[29] M. G. Albrow,[7] S. R. Amendolia,[25] D. Amidei,[18] J. Antos,[31] C. Anway-Wiese,[4] S. Aota,[34] G. Apollinari,[29] T. Asakawa,[34] W. Ashmanskas,[16] M. Atac,[7] F. Azfar,[24] P. Azzi-Bacchetta,[23] N. Bacchetta,[23] W. Badgett,[18] S. Bagdasarov,[29] M. W. Bailey,[20] J. Bao,[37] P. de Barbaro,[28] A. Barbaro-Galtieri,[16] V. E. Barnes,[27] B. A. Barnett,[14] E. Barzi,[8] G. Bauer,[17] T. Baumann,[10] F. Bedeschi,[25] S. Behrends,[3] S. Belforte,[25] G. Bellettini,[25] J. Bellinger,[36] D. Benjamin,[33] J. Benlloch,[17] J. Bensinger,[3] D. Benton,[24] A. Beretvas,[7] J. P. Berge,[7] J. Berryhill,[5] S. Bertolucci,[8] B. Bevensee,[24] A. Bhatti,[29] K. Biery,[13] M. Binkley,[7] D. Bisello,[23] R. E. Blair,[1] C. Blocker,[3] A. Bodek,[28] W. Bokhari,[17] V. Bolognesi,[2] G. Bolla,[23] D. Bortoletto,[27] J. Boudreau,[26] L. Breccia,[2] C. Bromberg,[19] N. Bruner,[20] E. Buckley-Geer,[7] H. S. Budd,[28] K. Burkett,[18] G. Busetto,[23] A. Byon-Wagner,[7] K. L. Byrum,[1] J. Cammerata,[14] C. Campagnari,[7] M. Campbell,[18] A. Caner,[25] W. Carithers,[16] D. Carlsmith,[36] A. Castro,[23] D. Cauz,[25] Y. Cen,[28] F. Cervelli,[25] P. S. Chang,[31] P. T. Chang,[31] H. Y Chao,[31] J. Chapman,[18] M.-T. Cheng,[31] G. Chiarelli,[25] T. Chikamatsu,[34] C. N. Chiou,[31] L. Christofek,[12] S. Cihangir,[7] A. G. Clark,[9] M. Cobal,[25] E. Cocca,[25] M. Contreras,[5] J. Conway,[30] J. Cooper,[7] M. Cordelli,[8] C. Couyoumtzelis,[9] D. Crane,[1] D. Cronin-Hennessy,[6] R. Culbertson,[5] T. Daniels,[17] F. DeJongh,[7] S. Delchamps,[7] S. Dell'Agnello,[25] M. Dell'Orso,[25] R. Demina,[7] L. Demortier,[29] B. Denby,[25] M. Deninno,[2] P. F. Derwent,[7] T. Devlin,[30] J. R. Dittmann,[6] S. Donati,[25] J. Done,[32] T. Dorigo,[23] A. Dunn,[18] N. Eddy,[18] K. Einsweiler,[16] J. E. Elias,[7] R. Ely,[16] E. Engels Jr.,[26] D. Errede,[12] S. Errede,[12] Q. Fan,[27] C. Ferretti,[25] I. Fiori,[2] B. Flaugher,[7] G. W. Foster,[7] M. Franklin,[10] M. Frautschi,[33] J. Freeman,[7] J. Friedman,[17] H. Frisch,[5] T. A. Fuess,[1] Y. Fukui,[15] S. Funaki,[34] G. Gagliardi,[25] S. Galeotti,[25] M. Gallinaro,[23] M. Garcia-Sciveres,[16] A. F. Garfinkel,[27] C. Gay,[10] S. Geer,[7] D. W. Gerdes,[14] P. Giannetti,[25] N. Giokaris,[29] P. Giromini,[8] G. Giusti,[25] L. Gladney,[24] D. Glenzinski,[14] M. Gold,[20] J. Gonzalez,[24] A. Gordon,[10] A. T. Goshaw,[6] K. Goulianos,[29] H. Grassmann,[25] L. Groer,[30] C. Grosso-Pilcher,[5] G. Guillian,[18] R. S. Guo,[31] C. Haber,[16] E. Hafen,[17] S. R. Hahn,[7] R. Hamilton,[10] R. Handler,[36] R. M. Hans,[37] K. Hara,[34] A. D. Hardman,[27] B. Harral,[24] R. M. Harris,[7] S. A. Hauger,[6] J. Hauser,[4] C. Hawk,[30] E. Hayashi,[34] J. Heinrich,[24] K. D. Hoffman,[27] M. Hohlmann,[5] C. Holck,[24] R. Hollebeek,[24] L. Holloway,[12] A. Hölscher,[13] S. Hong,[18] G. Houk,[24] P. Hu,[26] B. T. Huffman,[26] R. Hughes,[21] J. Huston,[19] J. Huth,[10] J. Hylen,[7] H. Ikeda,[34] M. Incagli,[25] J. Incandela,[7] G. Introzzi,[25] J. Iwai,[34] Y. Iwata,[11] H. Jensen,[7] U. Joshi,[7] R. W. Kadel,[16] E. Kajfasz,[23] H. Kambara,[9] T. Kamon,[32] T. Kaneko,[34] K. Karr,[35] H. Kasha,[37] Y. Kato,[22] T. A. Keaffaber,[27] L. Keeble,[8] K. Kelley,[17] R. D. Kennedy,[30] R. Kephart,[7] P. Kesten,[16] D. Kestenbaum,[10] R. M. Keup,[12] H. Keutelian,[7] F. Keyvan,[4] B. Kharadia,[12] B. J. Kim,[28] D. H. Kim,[7,*] H. S. Kim,[13] S. B. Kim,[18] S. H. Kim,[34] Y. K. Kim,[16] L. Kirsch,[3] P. Koehn,[28] K. Kondo,[34] J. Konigsberg,[10] S. Kopp,[5] K. Kordas,[13] A. Korytov,[17] W. Koska,[7] E. Kovacs,[7,*] W. Kowald,[6] M. Krasberg,[18] J. Kroll,[7] M. Kruse,[28] T. Kuwabara,[34] S. E. Kuhlmann,[1] E. Kuns,[30] A. T. Laasanen,[27] N. Labanca,[25] S. Lammel,[7] J. I. Lamoureux,[3] T. LeCompte,[1] S. Leone,[25] J. D. Lewis,[7] P. Limon,[7] M. Lindgren,[4] T. M. Liss,[12] N. Lockyer,[24] O. Long,[24] C. Loomis,[30] M. Loreti,[23] J. Lu,[32] D. Lucchesi,[25] P. Lukens,[7] S. Lusin,[36] J. Lys,[16] K. Maeshima,[7] A. Maghakian,[29] P. Maksimovic,[17] M. Mangano,[25] J. Mansour,[19] M. Mariotti,[23] J. P. Marriner,[7] A. Martin,[12] J. A. J. Matthews,[20] R. Mattingly,[17] P. McIntyre,[32] P. Melese,[29] A. Menzione,[25] E. Meschi,[25] S. Metzler,[24] C. Miao,[18] T. Miao,[7] G. Michail,[10] R. Miller,[19] H. Minato,[34] S. Miscetti,[8] M. Mishina,[15] H. Mitsushio,[34] T. Miyamoto,[34] S. Miyashita,[34] N. Moggi,[25] Y. Morita,[15] J. Mueller,[26] A. Mukherjee,[7] T. Muller,[4] P. Murat,[25] H. Nakada,[34] I. Nakano,[34] C. Nelson,[7] D. Neuberger,[4] C. Newman-Holmes,[7] M. Ninomiya,[34] L. Nodulman,[1] S. H. Oh,[6] K. E. Ohl,[37] T. Ohmoto,[11] T. Ohsugi,[11] R. Oishi,[34] M. Okabe,[34] T. Okusawa,[22] R. Oliveira,[24] J. Olsen,[36] C. Pagliarone,[2] R. Paoletti,[25] V. Papadimitriou,[33] S. P. Pappas,[37] N. Parashar,[25] S. Park,[7] A. Parri,[8] J. Patrick,[7] G. Pauletta,[25] M. Paulini,[16] A. Perazzo,[25] L. Pescara,[23] M. D. Peters,[16] T. J. Phillips,[6] G. Piacentino,[2] M. Pillai,[28] K. T. Pitts,[7] R. Plunkett,[7] L. Pondrom,[36] J. Proudfoot,[1] F. Ptohos,[10] G. Punzi,[25] K. Ragan,[13] D. Reher,[16] A. Ribon,[23] F. Rimondi,[2] L. Ristori,[25] W. J. Robertson,[6] T. Rodrigo,[25] S. Rolli,[25] J. Romano,[5] L. Rosenson,[17] R. Roser,[12] W. K. Sakumoto,[28] D. Saltzberg,[5] A. Sansoni,[8] L. Santi,[25] H. Sato,[34] P. Schlabach,[7] E. E. Schmidt,[7] M. P. Schmidt,[37] A. Scribano,[25] S. Segler,[7] S. Seidel,[20] Y. Seiya,[34] G. Sganos,[13] M. D. Shapiro,[16] N. M. Shaw,[27] Q. Shen,[27] P. F. Shepard,[26] M. Shimojima,[34] M. Shochet,[5] J. Siegrist,[16] A. Sill,[33] P. Sinervo,[13] P. Singh,[26] J. Skarha,[14] K. Sliwa,[35] F. D. Snider,[14] T. Song,[18] J. Spalding,[7] T. Speer,[9] P. Sphicas,[17] F. Spinella,[25] M. Spiropulu,[10] L. Spiegel,[7] L. Stanco,[23] J. Steele,[36] A. Stefanini,[25] K. Strahl,[13] J. Strait,[7] R. Ströhmer,[7,*] D. Stuart,[7] G. Sullivan,[5] A. Soumarokov,[31] K. Sumorok,[17] J. Suzuki,[34] T. Takada,[34] T. Takahashi,[22] T. Takano,[34] K. Takikawa,[34] N. Tamura,[11] F. Tartarelli,[25] W. Taylor,[13] P. K. Teng,[31] Y. Teramoto,[22] S. Tether,[17] D. Theriot,[7] T. L. Thomas,[20]

R. Thun,[18] M. Timko,[35] P. Tipton,[28] A. Titov,[29] S. Tkaczyk,[7] D. Toback,[5] K. Tollefson,[28] A. Tollestrup,[7]
J. F. de Troconiz,[10] S. Truitt,[18] J. Tseng,[14] T. Uchida,[34] N. Uemura,[34] F. Ukegawa,[24] G. Unal,[24] J. Valls,[7,*]
S. C. van den Brink,[26] S. Vejcik III,[18] G. Velev,[25] R. Vidal,[7] M. Vondracek,[12] D. Vucinic,[17] R. G. Wagner,[1]
R. L. Wagner,[7] J. Wahl,[5] N. Wallace,[25] C. Wang,[6] C. H. Wang,[31] J. Wang,[5] M. J. Wang,[31] Q. F. Wang,[29]
A. Warburton,[13] T. Watts,[30] R. Webb,[32] C. Wei,[6] C. Wendt,[36] H. Wenzel,[16] W. C. Wester III,[7] A. B. Wicklund,[1]
E. Wicklund,[7] R. Wilkinson,[24] H. H. Williams,[24] P. Wilson,[5] B. L. Winer,[21] D. Winn,[18] D. Wolinski,[18] J. Wolinski,[19]
S. Worm,[20] X. Wu,[9] J. Wyss,[23] A. Yagil,[7] W. Yao,[16] K. Yasuoka,[34] Y. Ye,[13] G. P. Yeh,[7] P. Yeh,[31] M. Yin,[6] J. Yoh,[7]
C. Yosef,[19] T. Yoshida,[22] D. Yovanovitch,[7] I. Yu,[7] L. Yu,[20] J. C. Yun,[7] A. Zanetti,[25] F. Zetti,[25] L. Zhang,[36]
W. Zhang,[24] and S. Zucchelli[2]

(CDF Collaboration)

[1]*Argonne National Laboratory, Argonne, Illinois 60439*
[2]*Istituto Nazionale di Fisica Nucleare, University of Bologna, I-40126 Bologna, Italy*
[3]*Brandeis University, Waltham, Massachusetts 02254*
[4]*University of California at Los Angeles, Los Angeles, California 90024*
[5]*University of Chicago, Chicago, Illinois 60637*
[6]*Duke University, Durham, North Carolina 27708*
[7]*Fermi National Accelerator Laboratory, Batavia, Illinois 60510*
[8]*Laboratori Nazionali di Frascati, Istituto Nazionale di Fisica Nucleare, I-00044 Frascati, Italy*
[9]*University of Geneva, CH-1211 Geneva 4, Switzerland*
[10]*Harvard University, Cambridge, Massachusetts 02138*
[11]*Hiroshima University, Higashi-Hiroshima 724, Japan*
[12]*University of Illinois, Urbana, Illinois 61801*
[13]*Institute of Particle Physics, McGill University, Montreal H3A 2T8
and University of Toronto, Toronto, Canada M5S 1A7*
[14]*The Johns Hopkins University, Baltimore, Maryland 21218*
[15]*National Laboratory for High Energy Physics (KEK), Tsukuba, Ibaraki 305, Japan*
[16]*Ernest Orlando Lawrence Berkeley National Laboratory, Berkeley, California 94720*
[17]*Massachusetts Institute of Technology, Cambridge, Massachusetts 02139*
[18]*University of Michigan, Ann Arbor, Michigan 48109*
[19]*Michigan State University, East Lansing, Michigan 48824*
[20]*University of New Mexico, Albuquerque, New Mexico 87131*
[21]*The Ohio State University, Columbus, Ohio 43210*
[22]*Osaka City University, Osaka 588, Japan*
[23]*Universita di Padova, Istituto Nazionale di Fisica Nucleare, Sezione di Padova, I-35131 Padova, Italy*
[24]*University of Pennsylvania, Philadelphia, Pennsylvania 19104*
[25]*Istituto Nazionale di Fisica Nucleare, University and Scuola Normale Superiore of Pisa, I-56100 Pisa, Italy*
[26]*University of Pittsburgh, Pittsburgh, Pennsylvania 15260*
[27]*Purdue University, West Lafayette, Indiana 47907*
[28]*University of Rochester, Rochester, New York 14627*
[29]*Rockefeller University, New York, New York 10021*
[30]*Rutgers University, Piscataway, New Jersey 08854*
[31]*Academia Sinica, Taiwan 11529, Republic of China*
[32]*Texas A&M University, College Station, Texas 77843*
[33]*Texas Tech University, Lubbock, Texas 79409*
[34]*University of Tsukuba, Tsukuba, Ibaraki 305, Japan*
[35]*Tufts University, Medford, Massachusetts 02155*
[36]*University of Wisconsin, Madison, Wisconsin 53706*
[37]*Yale University, New Haven, Connecticut 06511*
(Received 26 June 1996)

We have measured the cross section of $\gamma + D^{*\pm}$ production in $\bar{p}p$ collisions at $\sqrt{s} = 1.8$ TeV using the Collider Detector at Fermilab. In this kinematic region, the Compton scattering process ($g_c \rightarrow \gamma c$) is expected to dominate and thus provide a direct link to the charm quark density in the proton. From the 45 ± 18 $\gamma + D^{*\pm}$ candidates in a 16.4 pb^{-1} data sample, we have determined the production cross section to be 0.38 ± 0.15(stat) ± 0.11(syst) nb for the rapidity range $|y(D^{*\pm})| < 1.2$ and $|y(\gamma)| < 0.9$, and for the transverse momentum range $p_T(D^{*\pm}) > 6$ GeV/c and $16 < p_T(\gamma) < 40$ GeV/c. The measured cross section is compared to a theoretical prediction. [S0031-9007(96)01872-8]

In this Letter we report the first measurement of the production cross section for $\gamma + D^{*\pm}$ in $\bar{p}p$ collisions at $\sqrt{s} = 1.8$ TeV. Our previous direct photon measurements have concentrated on inclusive photon production and comparisons have been made to LO and NLO calculations [1]. Here, to further test QCD, we have taken the step of searching the inclusive photon sample for a more specific process: $\bar{p}p \to \gamma D^{*\pm}X$. Although the charm is not a particularly heavy quark, the photon + heavy quark (charm) predictions have been performed and are a topic of theoretical interest [2]. At LO, in the kinematic region covered by Collider Detector at Fermilab (CDF), the Compton process ($gc \to \gamma c$) is expected to dominate and thus provide a direct check of the charm quark density in the proton. A higher order calculation of the photon + charm process was recently completed [3]. In addition to a new test of QCD, measurement of the photon charm cross section provides important input to the production cross section estimations for current and future high energy hadron colliders.

The data used in this analysis were collected with the CDF detector during 1992–1993. Events containing a photon were selected by a trigger that required isolated clusters of electromagnetic energy with a 16 GeV transverse energy ($E_T = E\sin\theta$) threshold [1,4]. The proton fractional momentum $x = 2E_T/\sqrt{s}$ for this measurement covers the range $0.018 < x < 0.044$. This data sample contains approximately 800k events and corresponds to an integrated luminosity $\mathcal{L} = 16.4 \pm 0.6$ pb^{-1}.

The CDF detector is described in detail elsewhere [5]. Only the CDF detector systems relevant to this analysis are described here. Inside a 1.4 T solenoidal magnetic field, the silicon vertex detector (SVX), the vertex time projection chamber (VTX), and the central tracking chamber (CTC) provide the tracking and momentum information for charged particles. The SVX consists of four layers of silicon strip detectors and covers $|z| < 25$ cm. The VTX is used to measure the $\bar{p}p$ interaction vertex position along the z axis. The CTC is a cylindrical drift chamber consisting of 84 layers that are grouped into five axial and four stereo superlayers [6], and covering the pseudorapidity range $|\eta| < 1.2$. Located outside of the solenoid, the central electromagnetic calorimeter (CEM) has a projective tower geometry with a segmentation of $\Delta\phi \times \Delta\eta = 15° \times 0.11$ and covers $|\eta| < 1.1$. The central electromagnetic strip chamber (CES) is embedded in the CEM at the shower maximum position to measure electromagnetic shower profiles in both the ϕ and z directions.

Events with isolated photons were selected by the same cuts used in the CDF inclusive photon cross section measurement [1]. These cuts have a combined efficiency for selecting photons of 37% and include an isolation requirement of $E_T(0.7) < 2$ GeV, where $E_T(0.7)$ is the E_T sum (excluding the photon) in a cone of radius $R = \sqrt{(\Delta\eta)^2 + (\Delta\phi)^2} = 0.7$. We used photons within

the ranges $|y| < 0.9$ and $16 < p_T < 40$ GeV/c. The primary vertex of the $\bar{p}p$ interaction was required to be within $|z| < 60$ cm. If there were two or more primary vertices (multiple interactions) in an event, we selected the highest quality vertex by using the number of associated tracks and their fitting qualities [7]. The $D^{*\pm}$ candidates were required to come from this vertex. Approximately 110×10^3 events pass the cuts.

In these photon candidate events, we reconstructed $D^{*\pm}$ mesons using decays of $D^{*+} \to D^0\pi_s^+$ [8], $D^0 \to K^-\pi^+$ ($K\pi$), or $K^-\pi^+\pi^+\pi^-$ ($K3\pi$) and their charge conjugate modes. Hereafter charge conjugate modes are implied. We took all combinations of three (K-π-π_s) or five (K-π-π-π-π_s) tracks in an event to form a D^{*+} meson, preserving the electric charge correlation between the π_s^+ and K^- mesons. Tracks were required to include hits in two or more axial and in two or more stereo superlayers. The tracks were assumed to be alternatively a kaon or a pion, and were required to pass the kinematic cuts listed in Table I. The tracks forming a D^0 were constrained to come from a common point in space. The π_s^+ track was constrained to come from the primary vertex. The D^{*+} system was required to have $p_T > 6$ GeV/c to reduce the background due to random track combinations (combinatoric background). For each combination, we calculated the mass difference $\Delta m \equiv m(D^0\pi_s^+) - m(D^0)$. To prevent double counting, we chose the one D^0 combination whose reconstructed D^0 mass was closest to the world average D^0 mass ($= 1864.5$ MeV/c^2) [9]. If there were two or more D^{*+} combinations within $\Delta m < 168$ MeV/c^2 in an event, we selected the combination which had the highest D^{*+} p_T.

Two categories of backgrounds were considered in order to estimate the number of $\gamma + D^{*+}$ candidates: the photon background and the D^{*+} background. The fraction of the photons in the 110×10^3 photon sample was statistically determined by comparing the shower profile, as measured in the CES, with the profile expected from electron test beam data [10]; this is done for each Δm bin separately. The overall photon fraction for the sample is typical ($\sim 51\%$) of more general analyses [1].

Figure 1 shows the Δm distributions for the two combined D^0 decay channels and for a simulated D^{*+} background before subtracting photon backgrounds. The D^{*+} background was simulated using D^0 side band events within $60 < (m_{D^0} - 1864.5) < 120$ MeV/c^2. The

TABLE I. Kinematic cuts applied to tracks used in the D^{*+} reconstruction.

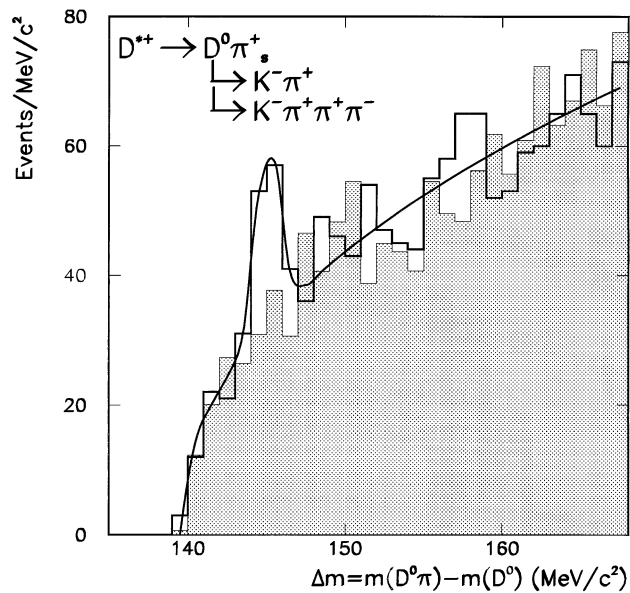|		$K\pi$	$K3\pi$	
p_T of K	>	1.0	1.7	GeV/c
Leading pion p_T	>	0.7	1.2	GeV/c
p_T of π's	>	$\cdots$	0.6	GeV/c
p_T of π_s^+	>	0.4	0.45	GeV/c
$|m_{D^0} - 1864.5|$	<	30	30	MeV/c^2

FIG. 1. The mass difference (Δm) distributions using the D^0 reconstructions of $D^0 \to K^- \pi^+$ and $D^0 \to K^- \pi^+ \pi^+ \pi^-$. The open histogram shows the data, and the shaded histrogram shows the D^{*+} background using the D^0 side band events. The solid line is the fit to the data described in the text.
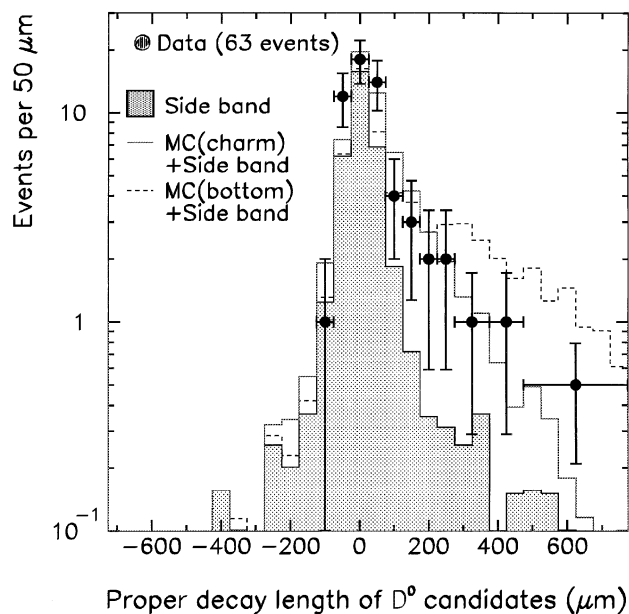

FIG. 2. The proper decay length distribution of the D^0 candidates in the $\gamma + D^{*+}$ events. The dots show the data where the errors on the data are statistical only. The shaded histrogram shows the background simulated by the side band events, and the solid and dashed lines show the distributions of the background plus Monte Carlo D^0 mesons originating from prompt c-quark hadronization and from b-quark decay, respectively.

number of background events was normalized to the data in $150 < \Delta m < 168$ MeV/c^2. A Gaussian distribution plus a simple background function $a \times (\Delta m - m_\pi)^b$ were fitted to the data, where m_π is the pion mass; the result of the fit is shown in the figure. The mean of the fitted Gaussian distribution was $\Delta m = (145.0 \pm 0.3)$ MeV/c^2, where the error is statistical only. This is consistent with the world average mass difference of $m_{D^*(2010)^+} - m_{D^0} = (145.42 \pm 0.05)$ MeV/c^2 [9]. The width, $\sigma_{\Delta m} = (0.7 \pm 0.2)$ MeV/c^2, is consistent with the expectation from a CDF detector simulation. To determine the $\gamma + D^{*+}$ cross section we define the signal region as $144 < \Delta m < 147$ MeV/c^2. The number of D^{*+} background events in this region is determined using the D^0 side band described above under the assumption that the D^{*+} background events have the same Δm distribution as these combinatoric background events. As shown in Fig. 1 we observe 151 candidate $\gamma + D^{*+}$ events on a combinatoric background of 99 events before the photon background subtraction. The probability that the combinatoric background would fluctuate to give this signal is 0.1%. After the photon background subtraction we observe 45 ± 18 $\gamma + D^{*+}$ candidates (99 ± 18 events on a combinatoric background of 54 events). The probability that the combinatoric + photon backgrounds would fluctuate to give this signal is 1.2%.

We looked at the proper decay length ($c\tau$) distribution of the D^0 candidates within our sample by selecting the mass difference window $144 < \Delta m < 147$ MeV/c^2. From a total of 151 events in this window, we required at least 2 (3) tracks to include SVX information for the $K\pi$ ($K3\pi$) channel, and observed 16 (47) events.

The $c\tau$ distribution for these 63 events is shown in Fig. 2 together with that for Monte Carlo simulated D^0 mesons originating from prompt c-quark hadronization, b-quark decay, and background events ($150 < \Delta m < 168$ MeV/c^2), where the normalization was determined from the Δm distribution. The $c\tau$ distribution observed in the data is consistent with that of the simulated D^0 mesons from the hadronization of directly produced c quarks.

The contributions to $\gamma + D^{*+}$ production from gluon splitting ($q\bar{q} \to \gamma g \to \gamma c\bar{c}$) and b-quark decay ($bg \to \gamma b \to \gamma cX$) processes were estimated using two Monte Carlo programs, PYTHIA [11] and HERWIG [12], each followed by a CDF detector simulation. The fraction of our candidates involving gluon splitting is estimated by both PYTHIA and HERWIG to be 7%. We have made an independent check of this fraction from the inclusive jet data sample in which we reconstructed D^{*+} mesons. Assuming all of the D^{*+} mesons came from gluon splitting, we estimate a $(12 \pm 4)\%$ contribution from gluon splitting in the photon sample, after correcting for the different gluon fractions in the two samples. The fraction of b-quark decay processes that contribute to the $\gamma + D^{*+}$ cross section is expected to be small [13]. Both Monte Carlo programs estimate this fraction to be only 3%. The contribution of $c\bar{c}$ pair production was studied using PYTHIA. We obtained an upper limit of 2% at 95% C.L. for the contribution to our $\gamma + D^{*+}$ candidate events.

To measure the cross section for the $\gamma + D^{*+}$ production, the reconstruction efficiency of $\gamma + D^{*+}$ events was determined using the PYTHIA Monte Carlo program and the data. Compton scattering, gluon splitting, and b-quark decay processes were all considered [14]. The trigger efficiency (ϵ_{trig}) for photons in the region of $p_T > 16$ GeV/c and $|y| < 0.9$ is 0.80 ± 0.03 [1,10]. This was obtained from electron events collected with a lower E_T trigger. The photon selection cut efficiency (ε_{sel}) is 0.37 ± 0.01 [1]. The D^{*+} detection efficiencies (ε_{rec}) are 0.46 ± 0.01 and 0.24 ± 0.01 for the $K\pi$ and $K3\pi$ channels. These were estimated from simulated and real events. Effects such as density of hits in the tracking devices (or possible correlations between the photon and D^{*+} selection) were measured by embedding tracks from simulated D^{*+} mesons in real photon events on the opposite side of photon candidates in azimuthal angle and randomly in $|y| < 1.2$. The overall efficiencies ($\varepsilon = \varepsilon_{\text{trig}} \times \varepsilon_{\text{sel}} \times \varepsilon_{\text{rec}}$) were estimated to be $\varepsilon_{K\pi} = 0.136 \pm 0.018$ and $\varepsilon_{K3\pi} = 0.071 \pm 0.011$ for the $K\pi$ and $K3\pi$ channels, respectively, where the errors quoted include systematic effects which are dominated by the tracking efficiency estimations.

The cross section was calculated using

$$\sigma(p\bar{p} \rightarrow \gamma D^{*+} X) = \frac{N(\gamma + D^{*+})}{B_{D^0 \pi_s}(\varepsilon_{K\pi} B_{K\pi} + \varepsilon_{K3\pi} B_{K3\pi})\mathcal{L}},$$

where $N(\gamma + D^{*+})$ is the number of the $\gamma + D^{*+}$ candidates, $B_{D^0 \pi_s}$ ($= 68.1 \pm 1.6\%$) denotes the branching ratio of the $D^{*+} \rightarrow D^0 \pi_s^+$ decay, $B_{K\pi}$ ($= 3.84 \pm 0.13\%$) denotes the branching ratio of the $D^0 \rightarrow K^- \pi^+$ decay, and $B_{K3\pi}$ ($= 7.5 \pm 0.4\%$) denotes the branching ratio of the $D^0 \rightarrow K^- \pi^+ \pi^+ \pi^-$ decay. We used the world average values [9] for the decay branching ratios. The $\gamma + D^{*+}$ production cross section is measured to be $0.38 \pm 0.15 \pm 0.11$ nb for the rapidity range $|y(D^{*+})| < 1.2$ and $|y(\gamma)| < 0.9$ and for the transverse momentum range $p_T(D^{*+}) > 6$ GeV/c and $16 < p_T(\gamma) < 40$ GeV/c, where the first uncertainty is statistical and the second is systematic.

The contributions to the systematic uncertainty are summarized in Table II. The uncertainty in subtracting the photon background was determined to be 9% by comparing the measured inclusive photon cross sections obtained by two different background subtraction schemes [1]. The uncertainty associated with the D^{*+} reconstruction includes the following effects: (1) the difference in the track environment around a D^{*+} between real data and simulated data; (2) the D^{*+} p_T spectrum difference due to fragmentation, renormalization scale, relative fraction of the processes involved (Compton scattering, gluon splitting, and b-quark decay), and parton distribution function models. Three different parton distribution functions were used to estimate the model dependence of the D^{*+} p_T spectrum: CTEQ2M [15], MRSD0′, and MRSD-′ [16]. The largest variation between these acceptance estimates was 4.7% ($K\pi$) and 5.3% ($K3\pi$). The uncertainty on

TABLE II. Systematic uncertainties on the cross section.

Source	Contribution
Luminosity	3.6%
γ background subtraction	9%
D^{*+} background subtraction	25%
Branching ratio of the D^{*+} decay	2.4%
Branching ratio of the D^0 decays	3.4%
Reconstruction efficiency	11%
Total systematic uncertainty	29%

the D^{*+} background subtraction (25%) comes from the variation allowed in the shape of the background Δm distribution and is dominated by the statistics on the D^0 side band events. The total systematic uncertainty is 29% on the measured cross section.

The measured cross section can be compared to a theoretical prediction calculated with PYTHIA including the Compton scattering, the gluon splitting, and the b-quark decay processes. The calculated cross sections with the parton distribution functions CTEQ2M, MRSD0′, and MRSD-′ were 0.21, 0.22, and 0.18 nb, respectively, where the photon p_T was taken as the renormalization and factorization scales. The PYTHIA prediction for the cross section is consistent with, although somewhat lower than, the measurement within the experimental uncertainties $0.38 \pm 0.15(\text{stat}) \pm 0.11(\text{syst})$ nb. The $\approx 1\sigma$ disagreement between the PYTHIA predictions and the measurement could be an indication that improvements in the theoretical predictions such as higher order effects or modifications to the charm quark density are needed. Studies underway using additional channels [17] and the most recent theoretical predictions [3] will provide more insight into this issue.

———

*Visitor.

[1] F. Abe *et al.,* Phys. Rev. Lett. **73**, 2662 (1994).

[2] R.S. Fletcher, F. Halzen, and E. Zas, Phys. Rev. Lett. B **221**, 403 (1989); M. Stratmann and W. Vogelsang, Phys. Rev. D **52**, 1535 (1995).

[3] E.L. Berger and L.E. Gordon, Phys. Rev. D **54**, 2279 (1996); B. Baily, E.L. Berger, and L.E. Gordon, in Proceedings of the DPF96 Meeting of the American Physical Society, Minneapolis, Minnesota, 1996 (to be published).

[4] At CDF, the z axis lies along the proton beam axis and its origin is the nominal center of the detector. θ indicates the polar angle, and ϕ indicates the azimuthal angle. The pseudorapidity η is defined as $\eta \equiv -\ln(\tan\frac{\theta}{2})$. y indicates the rapidity. p_T is the momentum transverse to beam direction.

[5] F. Abe *et al.,* Nucl. Instrum. Methods Phys. Res., Sect. A **271**, 387 (1988); F. Abe *et al.,* Fermilab Report No. Fermilab-Pub-94/024-E, 1994 (unpublished).

[6] F. Bedeshci *et al.,* Nucl. Instrum. Methods Phys. Res., Sect. A **268**, 50 (1988).

[7] F. Snider *et al.,* Nucl. Instrum. Methods Phys. Res., Sect. A **268**, 75 (1988).

[8] To distinguish this pion from the D^0 decay products, we denote it by the symbol π_s^+.

[9] For a review of particle properties, see L. Montanet *et al.,* Phys. Rev. D **50**, 1173 (1994), and 1995 off-year partial update for the 1996 edition.

[10] F. Abe *et al.,* Phys. Rev. D **48**, 2998 (1993).

[11] H. U. Bengtsson and T. Sjöstrand, Comput. Phys. Commun. **46**, 43 (1987); T. Sjöstrand and H. U. Bengtsson, Comput. Phys. Commun. **43**, 367 (1987); T. Sjöstrand,

Report No. CERN-TH 6488, 1992. We used version 5.6 of PYTHIA.

[12] G. Marchesini and B. Webber, Nucl. Phys. **B310**, 461 (1988).

[13] M. L. Mangano, in *Proceedings of the 9th Topical Workshop on Proton-Antiproton Collider Physics, Tsukuba, Japan, 1993,* edited by K. Kondo and S. Kim (Universal Academy Press, Tokyo, 1994), p. 118.

[14] In PYTHIA, the relative fraction of Compton scattering, gluon splitting, and b-quark decay processes was 0.88:0.08:0.04 within the ranges of $|y(D^{*+})| < 1.2$, $|y(\gamma)| < 0.9$, $p_T(D^{*+}) > 6$ GeV/c, and $16 < p_T(\gamma) < 40$ GeV/c. We used this for the efficiency calculation.

[15] J. Botts *et al.,* Phys. Lett. B **304**, 159 (1993).

[16] A. D. Martin, W. J. Stirling, and R. G. Roberts, Phys. Rev. D **50**, 6734 (1994).

[17] CDF Collaboration, R. Blair *et al.,* in *Proceedings of the 10th Topical Workshop on Proton-Antiproton Collider Physics, Batavia, Illinois, 1995,* edited by R. Raja and J. Yoh (AIP Press, Woodbury, N.Y., 1996.